Propulsion Systems for e-VTOL Aircraft

Technical Milestone Report

Jordan Eriksen

Supervised by: **Dr Sam Grimshaw** and **Dr James Taylor**

Introduction

Electric Vertical Take-Off and Landing (e-VTOL) market value is forecast to treble in between 2019 - 2024 [6]. All corners of the e-VTOL design space are being explored by various innovative companies, however there is a non-homogeneity in their design philosophies arising from the lack of understanding of what constitutes the most efficient design. One unknown is the most effective choice of propulsor, open-rotor propeller or ducted fan. Where a conventional propeller is resilient to variation in inlet conditions, a ducted fan produces higher thrust output for a given power. The design challenge is therefore to obtain the performance enhancements of a ducted fan whilst minimising the weight of the system without compromising stability in off nominal conditions. Martin 2004 [4] showed that reducing leading edge radius on the intake reduces pitching moment on the duct (thus improving stability) in the presence of a crosswind.

This report outlines the design process of a ducted fan and flying testbed. These are used to compare the performance of the ducted fan with a generic 10" model aircraft propeller (hereafter 'baseline propeller') and an APC 'Slow Flyer' (VTOL optimised) 10" propeller [1] (hereafter 'APC propeller').

Design and Experimental Method

2.1 Flying Testbed

Figure 1 shows a modular flying testbed (FTB), developed to enable in-flight analysis of fan performance for application driven testing. The modular design consists of a data management and flight control chassis with fixings for variable size arms and propulsor mountings. This enables various propulsors to be attached to the same chassis allowing fairest comparison of performance.

2.1.1 Modular Propulsors

Three different propulsors are to be tested: a generic model aircraft propeller, an APC VTOL optimised propeller and a custom ducted fan. In order to minimise the variation in configuration between propulsors, the arm attachment used for the propellers and the

ducted fan is the same. The propellers are mounted onto $750kv$ electric motors, themselves mounted to the arms via lightweight adaptors. This ensures the setup is the same for the baseline and APC propellers. The ducted fan is also driven by the same $750kv$ motors.

2.1.2 Data Collection

Mounted on the central chassis is a custom made sensor management system based on a Raspberry Pi 3+ (*RPi3*), shown in Fig. 1. This is integrated with 4 RPM sensors mounted on the propulsor arms and an extendable $8n$ ADC for up to 18bit resolution data input. This provides a capability to take pressure transducer readings from tappings on the ducted fan casing, allowing aerodynamic measurements to be taken. The *RPi3* is integrated with the flight control hardware for collection of power data and to provide position control assisted by 3-direction ultrasound proximity sensors (chassis frame of reference; forward, right and down directions).

2.1.3 Flight Control

Flight control is automated by the Holybro *Pixhawk 4* [3] flight hardware with accompanying PX4 autopilot firmware. Automated position control is managed by the *RPi3*, with both the *Pixhawk 4* and *RPi3* controlled by a WiFi enabled laptop running QGroundControl [2] for remote *Pixhawk 4* management and UNIX based *SSH* [7] for remote control of the *RPi3*.

Figure 1: Flying testbed with RPi3 sensor management board visible (green PCB)

$$M_f = \frac{C_T^{3/2}}{\sqrt{2}C_P} \tag{1}$$

$$M_f = \frac{T_T}{P}\sqrt{\frac{T_T}{2\rho A_x}} \tag{2}$$

$$M_f = \sqrt{2\sigma} \tag{3}$$

2.2 Fan Design

2.2.1 Objectives

The primary design objective is to minimise power requirement for static hover of the FTB. This is done by maximising the Figure of Merit, M_f (defined as in Eqn. 1 by Martin 2004 [4] and as in Eqn. 2 by Pereira 2008 [5]) whilst minimising propulsor weight. Equation 3 shows the relationship between M_f and the diffusion factor σ, which scales with vehicle weight, hence there is a trade-off.

2.2.2 Variables

Design variables are summarised in the table below. In order to simplify the problem, the turbomachinery design space is reduced to 2 DoF and is characterised by the coefficients ϕ, flow coefficient, and ψ, stage loading, leaving geometric and electrical variables r_c, r_h, and Ω floating (prior to application of constraints).

Variable	Definition
Flow coefficient	$\phi = V_x/U$
Stage loading	$\psi = \Delta p_0/(\frac{1}{2}\rho U^2)$
Diffusion ratio	$\sigma = A_e/A\ (= \phi^2/2\psi)$
Hub Radius	r_h
Casing Radius	r_c
Motor Speed	$\Omega\ (= V \cdot k_v)$

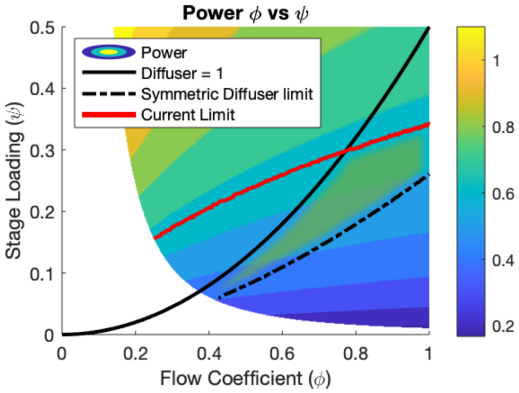

Figure 2: Non-Dim. Power requirement distribution. Green region shows limit of operation.

2.2.3 Constraints

Geometric constraints apply for r_h and r_c, arising from the outer radius of the chosen electric motor, and a maximum desired rotor size, respectively. A maximum value of r_c is chosen to be $100mm$ to ensure the design does not become cumbersome and can be rapidly prototyped.

2.2.4 Fixing Floating Variables

In addition to the objective of minimising power, weight is also to be minimised. A mass model, incorporated into a custom built analysis code, is used to determine that for a fixed M_f there is a trade-off between power and rotor radius (therefore weight). As thrust also scales with r_c, a minimum constraint on the variable r_c arises as *total vehicle weight* must equal *total thrust*. The custom built code calculates the power requirement (Fig. 2) at each design point, allowing a suitable operating point to be chosen.

2.3 Final Design Point Choice

In order to reduce exit kinetic energy losses, the flow coefficient is to be limited to a maximum value of 0.8. Therefore an operating point of $\phi = 0.8$, $\psi = 0.2$ and a nominal motor RPM of 7500 is chosen, with the mass model determining the required value of r_c. This operating point ensures the propulsor will remain within it's limits of operation when payload is increased. The operating point is summarised below.

Figure 3: Render of final ducted fan design, prior to prototyping

Flow coefficient	ϕ	0.8
Stage loading	ψ	0.2
Diffusion ratio	σ	1.26
Casing radius	r_c	57.7 mm
Figure of Merit	M_f	1.515

2.4 Determining Performance

Propulsor performance is assessed by determining power consumption for steady hover, and analysing the stability of the platform in off nominal inlet conditions, simulated by performing small amplitude horizontal manoeuvres.

2.4.1 Test 1: Static Hover

A propulsor is mounted on the FTB and a static hover test is undertaken in which the power required to maintain hover is determined. This test is repeated at varying payloads to assess the off design performance of the propulsor, and the resilience of this performance to changes in flow Reynolds number, Re, defined by

$$Re = \frac{\rho U c}{\mu} \tag{4}$$

where U is rotor (propeller or fan) midline speed and c is the rotor midline chord. In this test, total electrical power and total vehicle weight will be used in the determination of M_f (see Eqn. 2).

2.4.2 Test 2: Dynamic Stability

Resilience of the propulsor intake to off design conditions is assessed in two ways: examination of the aerodynamic behaviour of the intake and exit, and stability of the FTB during manoeuvres. The FTB undergoes small amplitude manoeuvres with no payload in a secured indoor test environment to simulate intake crosswinds and assess platform stability.

Experimental Results

The hardware required to undertake tests 1 and 2 is complete, however software alterations are required before test 2 can be conducted safely. At the time of writing, test 1 has begun data collection with data from the baseline propeller obtained.

3.1 Test 1: Static Hover

Below is the M_f obtained from the baseline propeller in the Re range $10,000 - 13,000$, presented alongside the theoretical maximum M_f for an open rotor propeller (1) and the predicted M_f for the ducted fan (1.52).

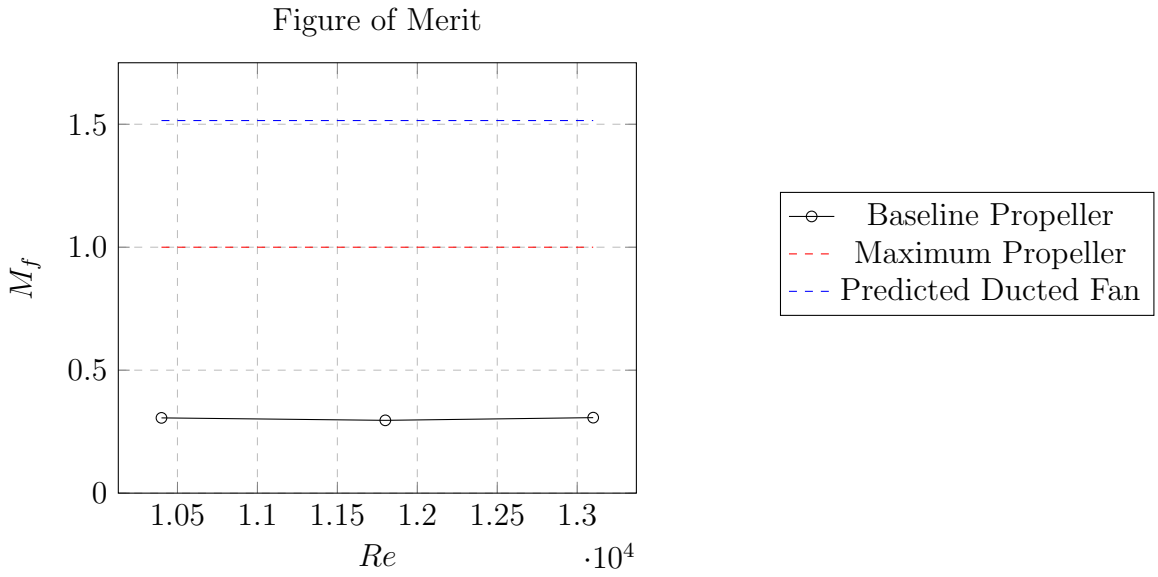

The data shows the propulsor to be insensitive to variations in Re between $10,000$ and $13,000$. The mean value of M_f obtained is about 0.3, 30% of the theoretical maximum for an open-rotor propeller. Data for the APC propeller and the ducted fan are to be collected next to compare performance to this baseline.

Conclusions

1. A modular flying testbed has been developed to enable:
   (a) calculation of a figure of merit in-flight;
   (b) determination of vehicle dynamic stability.
2. There is a trade-off between ducted fan mass and figure of merit in static hover, arising from the relationship $M_f = \sqrt{2\sigma}$.
3. A mass model is employed to optimise a light-weight ducted fan design for static hover. The ducted fan has a predicted figure of merit of 1.5.
4. Testing of a baseline propeller found a figure of merit of 0.3 corresponding to 30% of the theoretical maximum for an open-rotor propeller. This is insensitive to changes in Re in the range $10,000 - 13,000$.

Nomenclature

A		Flow Area at Rotor
A_E		Diffuser Exit Area
c		Rotor Midline Chord
e-VTOL		Electric Vertical Take-Off and Landing
FTB		Flying Testbed
h_0		Stagnation Enthalpy
M_f		Figure of Merit
Re		Reynolds Number
r_h		Fan Hub Radius
r_c		Fan Casing Radius
r_m		Fan Midline Radius
U	$= \Omega \cdot r_m$	Midline Fan Speed
V_x		Axial Flow Velocity
μ		Dynamic Viscosity of Air
ρ		Density of Air
σ	$= A_E/A$	Diffusion Factor
ϕ	$= V_x/U$	Flow Coefficient
ψ	$= \Delta h_0/U^2$	Stage Loading
Ω		Fan Speed

References

[1] Advanced Precision Composites. *APC Propeller Performance Data*. 2014. URL: `https://www.apcprop.com/files/PER3_10x47SF.dat` (visited on 19/12/2019).

[2] QGroundControl – Drone Control. *QGroundControl*. 2019. URL: `http://qgroundcontrol.com/` (visited on 07/01/2020).

[3] Holybro. *Pixhawk 4*. 2018. URL: `http://www.holybro.com/product/pixhawk-4/` (visited on 07/01/2020).

[4] Preston Martin and Chee Tung. *Performance and flowfield measurements on a 10-inch ducted rotor vtol uav*. Tech. rep. ARMY RESEARCH DEVELOPMENT and ENGINEERING COMMAND MOFFETT FIELD CA AVIATION ..., 2004.

[5] Jason L Pereira. *Hover and wind-tunnel testing of shrouded rotors for improved micro air vehicle design*. Tech. rep. MARYLAND UNIV COLLEGE PARK DEPT OF AEROSPACE ENGINEERING, 2008.

[6] Lukas Schroth. *The Drone Market 2019-2024: 5 Things You Need to Know*. 2019. URL: `https://www.droneii.com/the-drone-market-2019-2024-5-things-you-need-to-know` (visited on 03/01/2020).

[7] Inc. SSH Communications Security. *SSH (Secure Shell)*. 2019. URL: `https://www.ssh.com/ssh` (visited on 07/01/2020).